Origins of Incomplete Fusion Products and the Suppression of Complete Fusion in Reactions of ^{7}Li

K. J. Cook,* E. C. Simpson, L. T. Bezzina, M. Dasgupta, D. J. Hinde, K. Banerjee,†
A. C. Berriman, and C. Sengupta
Department of Nuclear Physics, Research School of Physics and Engineering, The Australian National University, Canberra ACT 2601, Australia

(Received 16 October 2018; revised manuscript received 8 February 2019; published 15 March 2019)

Above-barrier complete fusion involving nuclides with low binding energy is typically suppressed by 30%. The mechanism that causes this suppression, and produces the associated incomplete fusion products, is controversial. We have developed a new experimental approach to investigate the mechanisms that produce incomplete fusion products, combining singles and coincidence measurements of light fragments and heavy residues in $^{7}\mathrm{Li} + {}^{209}\mathrm{Bi}$ reactions. For polonium isotopes, the dominant incomplete fusion product, only a small fraction can be explained by projectile breakup followed by capture: the dominant mechanism is triton cluster transfer. Suppression of complete fusion is therefore primarily a consequence of clustering in weakly bound nuclei rather than their breakup prior to reaching the fusion barrier. This implies that suppression of complete fusion will occur in reactions of nuclides where strong clustering is present.

DOI: 10.1103/PhysRevLett.122.102501

Nuclear reactions occurring at energies near the fusion barrier are uniquely sensitive probes of the interplay between nuclear structure and dynamics. As more exotic weakly bound isotopes become accessible at new accelerator facilities, it is becoming critically important to understand the influence of weak binding on reaction dynamics, including on fusion. Fusion requires the system to overcome the barrier generated by the repulsive Coulomb and attractive nuclear potentials. A long-standing challenge in reactions involving light weakly bound stable nuclides (e.g., ^{6,7,8}Li, ^{9}Be) is that above-barrier complete fusion, experimentally defined as complete charge capture, is suppressed by ~30% relative to both calculations [1–16], and to measurements for comparable well-bound systems [2,3,8–10].

Suppression of complete fusion has been found to be associated with large yields of elements heavier than the target nucleus but lighter than the products of complete fusion [1,3,5,6,8,10,13,14,16]. These are usually called incomplete fusion products [1,17]. Crucially, their yields are comparable to the deficit in the complete fusion products, suggesting a common origin.

The degree of fusion suppression is strongly correlated [8] with the threshold for breakup of the light nucleus into its cluster constituents (e.g., $^{7}\mathrm{Li} \rightarrow \alpha + t$), suggesting that weak binding is the critical factor. This supported the suggestion that breakup into cluster constituents is the cause of both complete fusion suppression and incomplete fusion in reactions of weakly bound nuclei [1]. In this picture, disintegration into two charged fragments outside the fusion barrier may allow one (or both) fragments to escape, leading to a reduction of complete fusion. Here, incomplete fusion is interpreted as a two step process: breakup outside the barrier radius followed by capture of one of the fragments by the target (*breakup capture*).

To characterize the mechanisms leading to projectile breakup, much experimental work has focused on breakup at energies below the barrier V_b, where no charged particles are captured (*no-capture breakup*). A wide range of breakup modes have been identified for ^{6,7,8}Li and ^{9}Be, including direct breakup and transfer to neighboring unbound nuclides [18–22].

The amount of breakup capture occurring at above-barrier energies can then be estimated using classical trajectory models [23,24]. Some works have suggested that breakup capture fully accounts for the suppression of complete fusion [19,25,26]. However, when the characteristic timescales of breakup are treated explicitly, and model inputs carefully constrained by experimental results for no-capture breakup [22,27,28], the simulations account for only a small fraction of the measured incomplete fusion cross section [29]. There is, therefore, great uncertainty regarding the mechanism producing the majority of the incomplete fusion products, the cause of suppression of complete fusion, and the consequences for weakly bound unstable isotopes.

In this Letter, we present an innovative experimental approach to investigate the mechanisms leading to incomplete fusion products. Using a detector array with large angular coverage and high granularity, we measure the full distribution in energy and angle of the light reaction products associated with polonium isotopes, the dominant

incomplete fusion products [3]. We show that the majority cannot be produced by breakup followed by capture, and instead result from triton cluster transfer.

The experiments were conducted at the Australian National University Heavy Ion Accelerator Facility. Beams of ^{7}Li were delivered by the 14UD electrostatic accelerator, onto a 1.6 mg/cm^2 ^{209}Bi target oriented at 45° to the beam axis. Measurements were performed at a range of midtarget beam energies from $E_{\mathrm{c.m.}} = 30.42$ to 46.46 MeV (1.03 to 1.57 $E_{\mathrm{c.m.}}/V_b$ [3]), chosen to match existing polonium cross-section measurements [3]. The beam was pulsed with 0.8 ns FWHM bunches delivered every 535 ns. Reaction products were detected using two $\Delta E - E$ telescopes subtending 1.92 sr covering scattering angles $29° < \theta_{\mathrm{lab}} < 89°$ and $94° < \theta_{\mathrm{lab}} < 157°$ with azimuthal acceptance $107° < \phi < 176°$ and $185° < \phi < 254°$, respectively [30]. The telescopes consisted of 400 (ΔE) and 500 μm (E_{residual}) wedge-shaped double-sided silicon strip detectors, segmented into 16 arcs and 8 sectors. The geometry covered breakup fragment opening angles up to 163° [30]. Cross sections were normalized to Rutherford scattering measured using ion implanted detectors placed vertically above and below the beam axis at 17° [30].

Identification of prompt (beam-associated) particles was achieved via $\Delta E - E$, and by energy and time of flight (TOF). Low electronic noise levels allowed TOF separation of p, d, and t despite a flight path of typically only 10 cm. Decay α particles emitted isotropically from the ground state of ^{212}Po (295 ± 1 ns half-life [33]) were measured between beam bursts in coincidence with prompt α particles. Nearly all ^{212}Po nuclei stop in the target [30].

No-capture breakup was measured through detection of two prompt charged particles in coincidence. To overcome kinematic bias, double-differential cross sections $d^2\sigma/dEd\Omega$ for α arising from no-capture breakup were extracted using the efficiency correction procedure described in Ref. [29] using a classical dynamical model simulation [24] for each breakup mode [30]. At $E_{\mathrm{c.m.}} =$ 38.72 MeV, the no-capture breakup cross section of 36 ± 1 mb comprises almost equal components of direct breakup $^{7}\mathrm{Li} \rightarrow \alpha + t$ ($\sigma_{\alpha t} = 9.6 \pm 0.6$ mb), and breakup following one proton pickup $^{8}\mathrm{Be} \rightarrow \alpha + \alpha$ ($\sigma_{\alpha\alpha} = 7.3 \pm 0.4$ mb), one neutron stripping $^{6}\mathrm{Li} \rightarrow \alpha + d$ ($\sigma_{\alpha d} = 10.8 \pm 0.5$ mb), and two neutron stripping $^{5}\mathrm{Li} \rightarrow \alpha + p$ ($\sigma_{\alpha p} = 8.6 \pm 0.5$ mb). Of these, ∼16 mb of breakup occurs via long-lived ($\gtrsim 10^{-20}$ s) resonant states which cannot contribute to breakup capture [21,22,28,29]. For the remaining 20 mb, only a small fraction occurs faster than the fusion process ($<10^{-21}$ s) [22,29], and can thus contribute to the suppression of complete fusion. The fact that this cross section is so small, relative to that of incomplete fusion products (302 ± 21 mb at this energy [3]), is consistent with earlier work that concluded that breakup capture can explain only a small part of incomplete fusion [22,27,29,34]. This conclusion also applies at the other beam energies measured.

The double-differential cross section for all α particles arising from no-capture breakup (i.e., those accompanied by another prompt beamlike light charged fragment) can be found by summing the efficiency-corrected α-particle cross sections for all breakup modes. This is shown in Fig. 1(a). The projection onto angle, generating $d\sigma/d\Omega$, is shown by the blue points in Fig. 1(d). The data show a peak in yield near the grazing angle (dashed vertical line), taken to be where the ratio of elastic to Rutherford cross sections $d\sigma_{\mathrm{elas}}/d\sigma_{\mathrm{Ruth}} = 0.5$.

Polonium incomplete fusion products must be associated with an α particle that is not accompanied by another light charged fragment. The distribution in energy and angle of these "unaccompanied" α particles offers a direct probe of the polonium production mechanisms. The total α-particle distribution includes both unaccompanied α particles and α particles from no-capture breakup. Subtracting the efficiency-corrected no-capture breakup distribution [Fig. 1(a)] gives the unaccompanied α-particle distribution shown in Fig. 1(b), whose projection on angle ($d\sigma/d\Omega$) is shown in Fig. 1(d) by the orange points. The relative magnitudes of no-capture breakup and unaccompanied α-particle cross sections is consistent with previous work, where unaccompanied α particles were found to be the dominant contributor to the inclusive α-particle distribution [35,36]. The angle-integrated total unaccompanied α cross sections match well with measured polonium cross sections from Ref. [3] (discussed later) confirming the accuracy of the unaccompanied α cross sections.

The unaccompanied α-particle [1(b)] and no-capture breakup α [1(a)] spectra show several differences. The unaccompanied α particles (i) extend to much higher energies, (ii) exhibit a very different correlation in E_α and θ, (iii) have a much higher cross section at all angles, and (iv) peak at a more forward angle [Fig. 1(d)]. In particular, the latter would not be expected if breakup were responsible for producing the unaccompanied α particles. Breakup resulting in capture of one or more fragments will, on average, arise from more central collisions than those where none of the charged fragments are captured (i.e., no-capture breakup). The more central trajectories will naturally produce α particles at more backward angles, in contrast with the experimental results.

The idea that breakup capture should peak backward of no-capture breakup is confirmed by classical dynamical model simulations of breakup [24]. The simulation was constrained to reproduce the individual no-capture breakup total cross sections ($\sigma_{\alpha\alpha}$, $\sigma_{\alpha t}$, $\sigma_{\alpha d}$, $\sigma_{\alpha p}$) as well as the measured relative energy distributions of the breakup fragments [20,21,28]. The resulting simulated no-capture breakup double differential cross-section distribution as a function of energy and angle is shown in Fig. 1(c), and $d\sigma/d\Omega$ by the blue curve in panel (d). The experimental

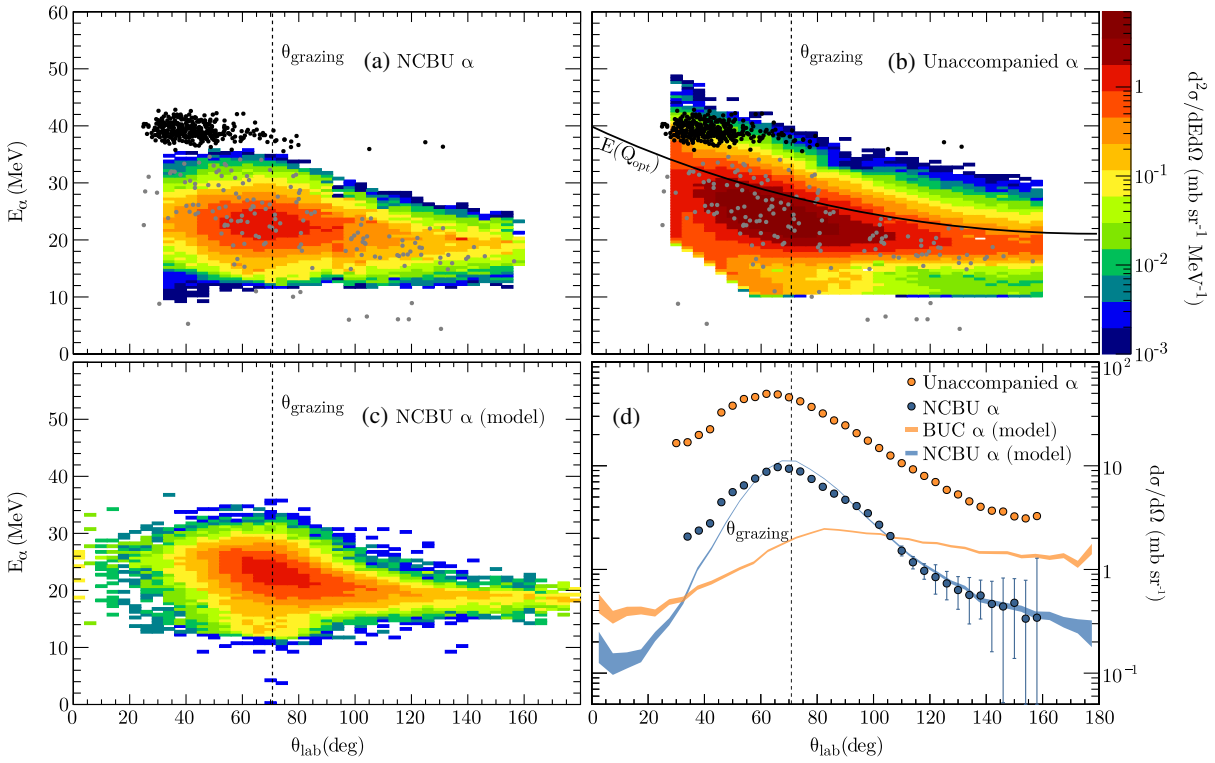

FIG. 1. Double differential cross sections $d^2\sigma/dEd\Omega(E_\alpha, \theta_{lab})$ for (a) α particles arising from no-capture breakup (NCBU) and (b) unaccompanied α particles in the reaction of ^{7}Li with ^{209}Bi at $E_{\mathrm{c.m.}} = 38.72$ MeV ($E_{\mathrm{c.m.}}/V_b = 1.31$). The angular distributions are continuous across the 5° gap between the detectors, because the 4° angular bin boundary was in the middle of the gap. A diagonal cut at low energy and angle has been applied in panel (b) to remove the known contribution of light impurities. The α detected in coincidence with ^{212}Po decays are indicated (event-by-event) by the dots in panels (a) and (b). Events below ~38 MeV (shown in grey) cannot be genuine: the corresponding excitation energy of ^{212}Po lies above its one-neutron separation energy $S_n = 6.01$ MeV. They are interpreted to be random coincidences. Model calculations (described in text) of the double-differential cross sections for no-capture breakup α at the same energy are shown in panel (c). All panels have the same cross-section color scale. Panel (d) shows the differential cross sections $d\sigma/d\Omega(\theta_{\mathrm{lab}})$ for unaccompanied α (orange points) and no-capture breakup α (blue points), compared to the model predictions of breakup capture (BUC) (orange curve) and from no-capture breakup (blue curve).

$d^2\sigma/dEd\Omega$ [Fig. 1(a)] and $d\sigma/d\Omega$ [blue points in panel (d)] are both well reproduced. The simulation predicts that the α particles resulting from breakup capture [orange curve in panel (d)] are peaked at more backward angles than the no-capture breakup, consistent with intuitive expectations. This conflicts with the measured unaccompanied α particles [orange points in panel (d)], indicating that they predominantly arise from a different mechanism. We note that the magnitude of the simulated breakup-capture cross section is sensitive to the details of the model inputs (e.g., timescales of breakup, reaction probability as a function of projectile-target distance, target excitation) which are difficult to constrain. However, the form of the angular distribution is much less sensitive to these inputs, and consistently peaks at more backward angles than the simulated no-capture breakup. While it is conceivable that breakup capture could explain some of the yield of unaccompanied α particles at very backward angles, the model indicates that breakup capture cannot explain the bulk of the distribution. The forward focusing also shows that complete fusion followed by α evaporation (expected to be almost isotropic) cannot be a significant contributor, consistent with experimental cross-bombardment results [3].

Having eliminated breakup capture, we return to the question: what is the process producing most of the unaccompanied α particles? A clue is provided by the energy and angle distribution of the events found to be in coincidence with ^{212}Po α decay [black dots in Figs. 1(a) and 1(b)]. They are clustered at forward angles, having a narrow range at large E_α, and lie completely outside the distribution from no-capture breakup. These kinematics indicate a direct reaction mechanism.

The Q-value spectra, reconstructed using the measured E_α and θ_{lab}, offers further insights. The Q-value spectrum of the unaccompanied α particles is shown in Fig. 2 by the orange points, and α particles measured in coincidence with ^{212}Po α decay are shown by the purple points. Their cross sections almost match the unaccompanied α yields. The slight reduction may result from undetected rapid α decay

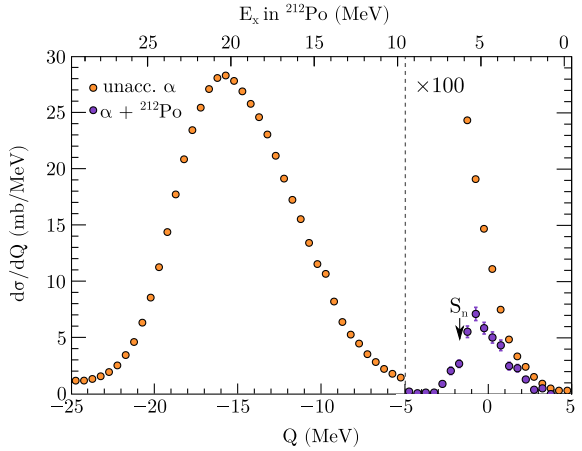

FIG. 2. Q value (bottom axis) and excitation energy E_x of ^{212}Po (top axis) distribution for unaccompanied α particles (orange) and α in coincidence with ^{212}Po α decay (purple) produced in reactions of ^{7}Li + ^{209}Bi at $E_{\mathrm{c.m.}} = 38.72$ MeV. The points have been multiplied by a factor of 100 for $Q > -5$ MeV to show the events in coincidence with ^{212}Po α decay. The one neutron separation energy of $S_n = 6.01$ MeV for ^{212}Po is indicated by the arrow.

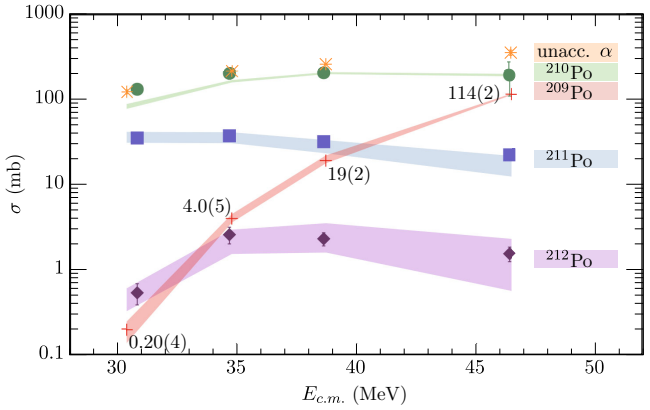

FIG. 3. Predicted (shaded curves) cross sections for various polonium isotopes from the measured unaccompanied α-excitation energy distribution folded with PACE4 calculations, compared to measured isotopic polonium cross sections (filled symbols) from α decay measurements [3]. The total unaccompanied α cross sections measured in the current work are indicated by the orange stars. The numbers along the band for ^{209}Po show the predicted values of the cross sections at the points indicated by the crosses.

from excited states of ^{212}Po during the beam-on period. The coincident α particles are associated with production of ^{212}Po at low excitation energy (top axis of Fig. 2), below the neutron separation energy $S_n = 6.01$ MeV.

The ^{212}Po yield *must* arise from direct triton cluster transfer from ^{7}Li, since the lowest possible excitation energy that can be populated by capture of a triton following breakup is the triton fusion Q value of 7.061 MeV. This would result in neutron emission, forming ^{211}Po rather than ^{212}Po.

The α particles measured in coincidence with ^{212}Po α decays form the tail of the much broader unaccompanied α Q-value distribution, as seen in Fig. 2. The dependence of α energy with angle, shown in Fig. 1(b), is consistent with that expected of an α particle produced at the optimum Q value, shown by the black line. Here, Q_{opt} has been calculated using the prescription of Ref. [37], which takes into account recoil effects. The total unaccompanied α distribution is therefore broadly consistent with production of ^{212}Po up to excitation energies of 28 MeV via triton cluster transfer.

Triton cluster transfer forming highly excited ^{212}Po will result in evaporation of neutrons, providing a mechanism for producing lighter polonium isotopes. Assuming all unaccompanied α particles are associated with production of ^{212}Po, the reconstructed excitation energy distribution for unaccompanied α particles can be used to calculate the cross sections of polonium isotopes using PACE4 statistical model calculations [38,39]. Probability distributions were generated for evaporated neutron multiplicities as a function of excitation energy and were folded with the deduced ^{212}Po excitation energy distribution to calculate the polonium cross sections. The chosen level density parameters $a_\nu = A/10$, and $a_f/a_\nu = 1.02$ reproduced the $1n$ and $2n$ evaporation cross sections from ^{208}Pb + $\alpha \rightarrow$ ^{212}Po fusion measurements of Refs. [40,41].

The resulting polonium cross sections following triton transfer are shown by the shaded bands in Fig. 3, along with the measured cross sections of Ref. [3] (filled symbols). The widths of the shaded bands indicate the uncertainty in the extrapolation of the experimental $d\sigma/d\Omega$ to angles forward of 28° and backward of 164° folded with the variation of the (unknown) angular momentum from $\ell = 0$ to $\ell = 5$. For comparison, the total unaccompanied α cross sections are indicated by the orange stars, which represent the expected total polonium cross section.

The cross sections for each polonium isotope determined through this procedure generally reproduce the measurements of Ref. [3] very well. The ^{210}Po cross sections from Ref. [3] may include contributions from incomplete fusion, direct proton transfer, and feeding from both ^{210}At ($Z = 2$ incomplete fusion) and ^{210}Bi (neutron stripping), which may account for the differences at low energy. The calculation also predicts the cross section of ^{209}Po, previously unmeasured due to the long half-life ($t_{1/2} = 124 \pm 3$ years). At $E_{\mathrm{c.m.}} = 46.46$ MeV, this isotope forms 35% of the total polonium yield, and is likely to contribute more than 50% at $E_{\mathrm{c.m.}} \gtrsim 50$ MeV. Cross-section measurements of ^{209}Po and ^{208}Po would allow testing of this model to higher energies.

The unaccompanied α particles, via their angular distribution, their energy-angle correlation, the deduced Q-value spectrum, and the predicted individual polonium cross sections, offer important new insights into the

mechanism leading to incomplete fusion products. In the present case of $^{7}\mathrm{Li} + ^{209}\mathrm{Bi}$, they are inconsistent with expectations of breakup followed by capture, and instead suggest a triton transfer mechanism. More generally, measurements of unaccompanied particle spectra, requiring comprehensive singles and coincidence measurements, offer a new and widely applicable approach to understand near-barrier fusion dynamics of weakly bound nuclei.

In summary, we have demonstrated characteristic differences between the energy-angle correlations for α particles from no-capture breakup and those associated with incomplete fusion products (unaccompanied α). The unaccompanied α particles peak forward of the no-capture breakup, inconsistent with expectations for breakup capture. We have unambiguously identified that ^{212}Po is produced by direct triton cluster transfer, and demonstrated that the measured distributions of all unaccompanied α particles are broadly consistent with triton transfer. This is the first time that the dominant mechanism resulting in incomplete fusion products has been clearly identified. Assuming ^{212}Po production by triton transfer followed by neutron evaporation, our results are in good agreement with the magnitude and energy dependence of previously measured polonium incomplete fusion cross sections [3].

Incomplete fusion products and the suppression of complete fusion have the same underlying cause. Weak binding leads to strong clustering, and greater displacement of those clusters from the projectile's center of mass. This makes the triton amenable to transfer [42], and requires the center of mass of the ^{7}Li projectile to get closer to the target to ensure that the entire projectile fuses. The former leads to incomplete fusion, and the latter to suppression of complete fusion. This interpretation should be valid for any nuclides that exhibit strong clustering.

To establish the systematics of this effect, above-barrier no-capture breakup and singles α yields of reactions of ^{6,7}Li and ^{9}Be on a range of targets will be valuable. The cross sections for complete and incomplete fusion products in reactions of exotic nuclei, such as ^{6}He, ^{8}Li, and ^{7,10,11}Be [12], will also provide very interesting insights into near-barrier reaction dynamics.

This work was supported by the Australian Research Council Grants No. DP170102423, No. DP160101254, and No. DP170102318. Support for ANU Heavy Ion Accelerator Facility operations through the NCRIS program is acknowledged. The authors thank M. A. Stoyer for his assistance during the experiment.

K. J. C and E. C. S. contributed equally to this work.

*kaitlin.cook@alumni.anu.edu.au
Present address: Department of Physics, Tokyo Institute of Technology, 2-12-1 O-Okayama, Meguro, Tokyo 152-8551, Japan.

†On leave from Variable Energy Cyclotron centre, 1/AF, Bidhan Nagar, Kolkata 700064, India.

[1] M. Dasgupta, D. J. Hinde, R. D. Butt, R. M. Anjos, A. C. Berriman, N. Carlin, P. R. S. Gomes, C. R. Morton, J. O. Newton, A. Szanto de Toledo, and K. Hagino, Phys. Rev. Lett. **82**, 1395 (1999).

[2] C. Signorini, Z. Liu, Z. Li, K. Löbner, L. Müller, M. Ruan, K. Rudolph, F. Soramel, C. Zotti, A. Andrighetto, L. Stroe, A. Vitturi, and H. Zhang, Eur. Phys. J. A **5**, 7 (1999).

[3] M. Dasgupta, P. R. S. Gomes, D. J. Hinde, S. B. Moraes, R. M. Anjos, A. C. Berriman, R. D. Butt, N. Carlin, J. Lubian, C. R. Morton, J. O. Newton, and A. Szanto de Toledo, Phys. Rev. C **70**, 024606 (2004).

[4] C. Signorini, T. Glodariu, Z. H. Liu, M. Mazzocco, M. Ruan, and F. Soramel, Prog. Theor. Phys. Suppl. **154**, 272 (2004).

[5] A. Mukherjee, S. Roy, M. Pradhan, M. Saha Sarkar, P. Basu, B. Dasmahapatra, T. Bhattacharya, S. Bhattacharya, S. Basu, A. Chatterjee, V. Tripathi, and S. Kailas, Phys. Lett. B **636**, 91 (2006).

[6] P. R. S. Gomes, I. Padron, E. Crema, O. A. Capurro, J. O. Fernández Niello, A. Arazi, G. V. Martí, J. Lubian, M. Trotta, A. J. Pacheco, J. E. Testoni, M. D. Rodríguez, M. E. Ortega, L. C. Chamon, R. M. Anjos, R. Veiga, M. Dasgupta, D. J. Hinde, and K. Hagino, Phys. Rev. C **73**, 064606 (2006).

[7] E. F. Aguilera, E. Martinez-Quiroz, P. Rosales, J. J. Kolata, P. A. DeYoung, G. F. Peaslee, P. Mears, C. Guess, F. D. Becchetti, J. H. Lupton, and Y. Chen, Phys. Rev. C **80**, 044605 (2009).

[8] L. R. Gasques, D. J. Hinde, M. Dasgupta, A. Mukherjee, and R. G. Thomas, Phys. Rev. C **79**, 034605 (2009).

[9] P. K. Rath, S. Santra, N. L. Singh, R. Tripathi, V. V. Parkar, B. K. Nayak, K. Mahata, R. Palit, S. Kumar, S. Mukherjee, S. Appannababu, and R. K. Choudhury, Phys. Rev. C **79**, 051601 (2009).

[10] C. S. Palshetkar, S. Santra, A. Chatterjee, K. Ramachandran, S. Thakur, S. K. Pandit, K. Mahata, A. Shrivastava, V. V. Parkar, and V. Nanal, Phys. Rev. C **82**, 044608 (2010).

[11] V. V. Parkar, R. Palit, S. K. Sharma, B. S. Naidu, S. Santra, P. K. Joshi, P. K. Rath, K. Mahata, K. Ramachandran, T. Trivedi, and A. Raghav, Phys. Rev. C **82**, 054601 (2010).

[12] D. J. Hinde and M. Dasgupta, Phys. Rev. C **81**, 064611 (2010).

[13] P. R. S. Gomes, R. Linares, J. Lubian, C. C. Lopes, E. N. Cardozo, B. H. F. Pereira, and I. Padron, Phys. Rev. C **84**, 014615 (2011).

[14] N. T. Zhang, Y. D. Fang, P. R. S. Gomes, J. Lubian, M. L. Liu, X. H. Zhou, G. S. Li, J. G. Wang, S. Guo, Y. H. Qiang, Y. H. Zhang, D. R. Mendes Junior, Y. Zheng, X. G. Lei, B. S. Gao, Z. G. Wang, K. L. Wang, and X. F. He, Phys. Rev. C **90**, 024621 (2014).

[15] L. Canto, P. R. S. Gomes, R. Donangelo, J. Lubian, and M. Hussein, Phys. Rep. **596**, 1 (2015).

[16] Y. D. Fang, P. R. S. Gomes, J. Lubian, M. L. Liu, X. H. Zhou, D. R. Mendes Junior, N. T. Zhang, Y. H. Zhang, G. S. Li, J. G. Wang, S. Guo, Y. H. Qiang, B. S. Gao, Y. Zheng, X. G. Lei, and Z. G. Wang, Phys. Rev. C **91**, 014608 (2015).

[17] K. Siwek-Wilczyńska, J. du Marchie van Voorthuysen, E. H. van Popta, R. Siemssen, and J. Wilczyński, Phys. Rev. Lett. **42**, 1599 (1979).
[18] A. Shrivastava, A. Navin, N. Keeley, K. Mahata, K. Ramachandran, V. Nanal, V. V. Parkar, A. Chatterjee, and S. Kailas, Phys. Lett. B **633**, 463 (2006).
[19] R. Rafiei, R. du Rietz, D. H. Luong, D. J. Hinde, M. Dasgupta, M. Evers, and A. Diaz-Torres, Phys. Rev. C **81**, 024601 (2010).
[20] D. H. Luong, M. Dasgupta, D. J. Hinde, R. Du Rietz, R. Rafiei, C. J. Lin, M. Evers, and A. Diaz-torres, Phys. Lett. B **695**, 105 (2011).
[21] D. H. Luong, M. Dasgupta, D. J. Hinde, R. du Rietz, R. Rafiei, C. J. Lin, M. Evers, and A. Diaz-Torres, Phys. Rev. C **88**, 034609 (2013).
[22] K. J. Cook, I. P. Carter, E. C. Simpson, M. Dasgupta, D. J. Hinde, L. T. Bezzina, S. Kalkal, C. Sengupta, C. Simenel, B. M. A. Swinton-Bland, K. Vo-Phuoc, and E. Williams, Phys. Rev. C **97**, 021601(R) (2018).
[23] A. Diaz-Torres, D. J. Hinde, J. A. Tostevin, M. Dasgupta, and L. R. Gasques, Phys. Rev. Lett. **98**, 152701 (2007).
[24] E. C. Simpson, K. J. Cook, S. Kalkal, D. H. Luong, I. P. Carter, M. Dasgupta, and D. J. Hinde, EPJ Web Conf. **163**, 00056 (2017).
[25] A. Shrivastava, A. Navin, A. Diaz-Torres, V. Nanal, K. Ramachandran, M. Rejmund, S. Bhattacharyya, A. Chatterjee, S. Kailas, A. Lemasson, R. Palit, V. Parkar, R. Pillay, P. Rout, and Y. Sawant, Phys. Lett. B **718**, 931 (2013).
[26] A. Diaz-Torres and D. Quraishi, Phys. Rev. C **97**, 024611 (2018).
[27] E. C. Simpson, K. J. Cook, D. H. Luong, Sunil Kalkal, I. P. Carter, M. Dasgupta, D. J. Hinde, and E. Williams, Phys. Rev. C **93**, 024605 (2016).
[28] Sunil Kalkal, E. C. Simpson, D. H. Luong, K. J. Cook, M. Dasgupta, D. J. Hinde, I. P. Carter, D. Y. Jeung, G. Mohanto, C. S. Palshetkar, E. Prasad, D. C. Rafferty, C. Simenel, K. Vo-Phuoc, E. Williams, L. R. Gasques, P. R. S. Gomes, and R. Linares, Phys. Rev. C **93**, 044605 (2016).
[29] K. J. Cook, E. C. Simpson, D. H. Luong, S. Kalkal, M. Dasgupta, and D. J. Hinde, Phys. Rev. C **93**, 064604 (2016).
[30] See Supplemental Material at http://link.aps.org/supplemental/10.1103/PhysRevLett.122.102501, which includes Refs. [31,32] for a description of the efficiency evaluation of the coincidence data.
[31] F. C. Barker, Aust. J. Phys. **41**, 743 (1988).
[32] A. M. Lane and R. G. Thomas, Rev. Mod. Phys. **30**, 257 (1958).
[33] G. Bellini *et al.*, Eur. Phys. J. A **49**, 92 (2013).
[34] H. D. Marta, L. F. Canto, and R. Donangelo, Phys. Rev. C **89**, 034625 (2014).
[35] S. K. Pandit, A. Shrivastava, K. Mahata, V. V. Parkar, R. Palit, N. Keeley, P. C. Rout, A. Kumar, K. Ramachandran, S. Bhattacharyya, V. Nanal, C. S. Palshetkar, T. N. Nag, S. Gupta, S. Biswas, S. Saha, J. Sethi, P. Singh, A. Chatterjee, and S. Kailas, Phys. Rev. C **96**, 044616 (2017).
[36] S. Santra, S. Kailas, V. V. Parkar, K. Ramachandran, V. Jha, A. Chatterjee, P. K. Rath, and A. Parihari, Phys. Rev. C **85**, 014612 (2012).
[37] J. P. Schiffer, H. J. Kijrner, R. H. Siemssen, K. W. Jones, and A. Schwarzschild, Phys. Lett. B **44**, 47 (1973).
[38] O. B. Tarasov and D. Bazin, Nucl. Instrum. Methods Phys. Res., Sect. B **266**, 4657 (2008).
[39] A. Gavron, Phys. Rev. C **21**, 230 (1980).
[40] A. R. Barnett and J. S. Lilley, Phys. Rev. C **9**, 2010 (1974).
[41] S. M. Lukyanov, Y. E. Penionzhkevich, R. A. Astabatian, N. A. Demekhina, Z. Dlouhy, M. P. Ivanov, R. Kalpakchieva, A. A. Kulko, E. R. Markarian, V. A. Maslov, R. V. Revenko, N. K. Skobelev, V. I. Smirnov, Y. G. Sobolev, W. Trazska, and S. V. Khlebnikov, Phys. Lett. B **670**, 321 (2009).
[42] J. Lei and A. M. Moro, Phys. Rev. Lett. **122**, 042503 (2019).